Polymer Journal, Vol. 3, No. 2, pp 140—148 (1972)

Light-Scattering Patterns from Random Assembly of Anisotropic Rods of Finite Dimensions*

Norio HAYASHI and Hiromichi KAWAI**

Department of Polymer Chemistry, Faculty of Engineering, Kyoto University, Kyoto, Japan.

(Received May 12, 1971)

ABSTRACT: The polarized light-scattering from a random assembly of anisotropic rods was formulated in three dimensions so that the size of the rod was finite in length as well as in radius, and that the principal optical axes of scattering elements were oriented within the rod with given polar and azimuthal angles to the rod axis.

The H_v and V_v scattering patterns were calculated by fixing either the length or radius of the rod as several times larger than the wave length, but, in contrast, varying either the radius or length of the rod from infinitesimally thin to the same order as the fixed length or radius, respectively, to include the infinitesimally thin rod or disc as extreme.

The H_v and V_v patterns degenerated, in general, into small scattering angles with the increasing of the radius or thickness of the infinitesimally thin rod or disc. The H_v patterns changed from $\times$-type to $+$-type patterns with the variations of the inclined angle of the scattering elements from zero to 50°, irrespective of the rod and disc models. On the other hand, however, the V_v patterns changed from the horizontal dumb-bell type to the vertical type for the rod model and from the vertical dumb-bell type to the horizontaltype for the disc model, both with the variations of the inclined angle from zero to 90°.

KEY WORDS Polarized Light Scattering / Anisotropic Rod of Finite Dimensions / Random Assembly Model / Calculations /

The small angle light-scattering patterns from film specimens of some particular polymers, such as polytetrafluoroethylene,[1] native cellulose,[2] collagen,[3] and amylose,[4] have been found to be quite different from those of film specimens of poly-alphaolefins having spherulitic crystalline textures.[5–8]

Stein, *et al.*, have explained this type of characteristic pattern from polytetrafluoroethylene film in terms of a random assembly of anisotropic rods in two dimensions,[1,9] while the present authors have extended Stein's formulation for the two dimensions to three dimensions for the pattern from collagen film,[3] assuming both the rod to be finite in length but infinitesimally thin in radius, and the principal optical axes of scattering elements to be oriented within the rod with given polar and azimuthal angles to the rod axis. On the other hand, van Aartsen has also formulated this type of characteristic pattern in terms of a random assembly of anisotropic rods in three dimensions, assuming the rod to be finite in length as well as in radius but the principal optical axes of the scattering elements to be parallel to the rod axis.[10]

In this paper, one of the more generalized formulations for this type of light-scattering pattern will be proposed by combining the former formulation by the present authors with that by van Aartsen; *i.e.*, a random assembly of anisotropic rods in three dimensions, assuming the rod to be finite in length as well as in radius and the principal optical axes of the scattering elements to be oriented within the rod with given polar and azimuthal angles to the rod axis. Any orientation distribution of the scattering elements within the rod will not be taken into consideration for the purpose of avoiding complexity of the calculations, and this type of further gen-

* Presented at the 20th Annual Meeting of the Society of Polymer Science, Japan, Tokyo, May 27, 1971.

** To whom every correspondence should be dressed.

eralization will be discussed in future.

Calculations

Figure 1 shows a schematic diagram of the coordinates system of light-sattering from an anisotropic rod having definite size of R in radius

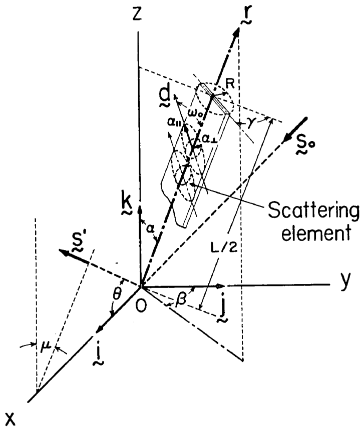

Figure 1. Schematic diagram showing the coordinates system of light scattering from the three-dimensional assembly model of anisotropic rods of finite dimensions.

and of L in length. The orientation of the rod is represented in terms of three Euler angles, β, α, and γ, with respect to the Cartesian coordinates, 0-xyz, where α and β are the polar and azimuthal angles, respectively, for defining the orientation of the rod axis of vector $\boldsymbol{r}$, while γ is the angle between the axis of symmetry of the rod and the plane including $0z$-axis and the rod axis for defining the rotation of the rod around its own rod axis. The Cartesian coordinates are fixed within the film specimen so that the $0x$-axis having its own unit vector $\boldsymbol{i}$ is taken as the film normal, and the $0y$- and $0z$-axes, whose respective unit vectors are $\boldsymbol{j}$ and $\boldsymbol{k}$, parallel to the film surface. The incident beam having unit vector $\boldsymbol{s}_0$ propagates along the $0x$-axis, *i.e.*, $\boldsymbol{s}_0=\boldsymbol{i}$, and its polarization direction, whose unit vector $\boldsymbol{e}$, is taken as parallel to the $0z$-axis to give $\boldsymbol{e}=\boldsymbol{k}$.

A unit vector $\boldsymbol{s}'$ along the scattered ray can be given by

$$\boldsymbol{s}'=\cos\theta\boldsymbol{i}+\sin\theta\sin\mu\boldsymbol{j}+\sin\theta\cos\mu\boldsymbol{k} \qquad (1)$$

where θ and μ are scattering and azimuthal angles of the scattered ray with respect to the $0x$- and $0z$-axes, respectively. The scattering vector $\boldsymbol{s}$, defined by $\boldsymbol{s}=(\boldsymbol{s}_0-\boldsymbol{s}')$, is given by

$$\boldsymbol{s}=(\boldsymbol{s}_0-\boldsymbol{s}')=(1-\cos\theta)\boldsymbol{i} \\ -\sin\theta\sin\mu\boldsymbol{j}-\sin\theta\cos\mu\boldsymbol{k} \qquad (2)$$

As assumed in a previous paper,[3] uniaxially polarizable elements having principal polarizabilities of $\alpha_{//}$ and $\alpha_\perp$, are oriented side-by-side within the rod with a given inclined angle ω_0 with respect to the rod axis; *i.e.*, every unit vector $\boldsymbol{d}$ along the rotational axes of the elements, and consequently, the direction of the principal polarizability $\alpha_{//}$, is laid parallel to the plane including the rod axis and the symmetric axis of the rod, as illustrated in Figure 1, with a common polar angle ω_0 and zero azimuthal angle with respect to the rod axis. Denoting (i) the difference between the polarizability along the element axis and the polarizability of the medium in which the rods are embedded, $b_r=(\alpha_{//}-\alpha_s)$, and (ii) the difference between the polarizability perpendicular to the element axis and the polarizability of the medium, $b_t=(\alpha_\perp-\alpha_s)$, then the induced dipole moment due to the radiation of the incident beam may be given by

$$\boldsymbol{M}=E_0\{\delta(\boldsymbol{e}\cdot\boldsymbol{d})\boldsymbol{d}+b_t\boldsymbol{e}\} \qquad (3)$$

where E_0 is the amplitude of the incident beam and $\delta=(b_r-b_t)$.

The amplitude of the scattered ray from the scattering elements within the rod may be given by

$$E=K\int_v(\boldsymbol{M}\cdot\boldsymbol{o})\cos k(\boldsymbol{r}\cdot\boldsymbol{s})\,\mathrm{d}\boldsymbol{r} \qquad (4)$$

where K is a constant, $\boldsymbol{o}$ is a unit vector along the polarization direction of the analyzer, $k=2\pi/\lambda'$, λ' is the wave length of the light within the specimen, and v means the integration to be performed over the entire volume of the rod. This volume integral is in contrast to the line integral in a previous paper in which the rod was assumed to be definite in length but infinitesimally thin in radius.

Further, assuming the rods to be oriented randomly within the space of the specimen with a distribution density N_0 per unit solid angle; *i.e.*, a random distribution of the three Euler angles,

β, α, and γ, for the orientation of the rods with respect to the Cartesian coordinates 0-xyz, the intensity distribution of the scattered light from the three-dimensional random assembly of the rods may be given by

$$I=(N_0/2)\int_0^{2\pi}\int_0^{2\pi}\int_0^{\pi}(\boldsymbol{M}\cdot\boldsymbol{o})^2\left[\int_v \cos k(\boldsymbol{r}\cdot\boldsymbol{s})\,\mathrm{d}\boldsymbol{r}\right]^2 \times \sin\alpha \mathrm{d}\alpha \mathrm{d}\beta \mathrm{d}\gamma \quad (5)$$

From the above equations, the intensity distribution of scattered light under H_v and V_v polarizations can be obtained by replacing $\boldsymbol{o}$ with $\boldsymbol{j}$ and $\boldsymbol{k}$, respectively, to give the same results as eq 6 and 7 in a previous paper with the exception of replacing A, B, and C in eq 9 through 11 also in the previous paper with D_2, D_1, and D_0, respectively, which are given in general form as

$$D_x=\frac{2\pi}{4\pi\cdot 2\pi}\int_0^{\pi}\cos^{2x}\alpha\int_0^{2\pi}\left[(1/v_{\mathrm{r}})\int_v \cos k(\boldsymbol{r}\cdot\boldsymbol{s})\mathrm{d}\boldsymbol{r}\right]^2 \times \mathrm{d}\gamma \sin\alpha \mathrm{d}\alpha \quad (6)$$

where v_{r} is the volume of the rod.

When performing the integration within the brackets in eq 6 in terms of cylindrical coordinates, as proposed by van Aartsen,[10] D_x can be given in the form of a series expansion as follows:

$$D_x=4\sum_{n=0}^{\infty}(-1)^n\frac{(hL)^{2n}}{(2n+2)!} \times\sum_{k=0}^{\infty}(-1)^k\frac{(hR)^{2k}}{(k+1)!(k+2)!} \times\frac{\Gamma(k+3/2)\Gamma(n+x+1/2)}{\Gamma(1/2)\Gamma(n+x+k+3/2)} \quad (7)$$

where h is a scattering angle defined by $(4\pi/\lambda')\times\sin(\theta/2)$.

As discussed in a previous paper, the shape of, for example, the H_v pattern has, in general, a four-fold symmetry with respect to the azimuthal angle μ, which changes from $\times$-type pattern to circular pattern to $+$-type pattern depending mostly on whether the value of the fourth order Legendre function $P_4(\cos\omega_0)$ takes positive, zero, or negative values, respectively. But, in detail, especially when the size of the rod is assumed to be finite in length as well as in radius, the type of the pattern must also depend on the value of $A(U)$, which has been defined by eq 9 in a previous paper and is given in terms of D_k as

$$A(U)=(35D_2-30D_1+3D_0) \quad (8)$$

In the following section, the effects of $A(U)$ upon the shape of the polarized light-scattering patterns, which have not been discussed in a previous paper with any more detail than keeping the length of the infinitesimally thin rod constant, will be checked in terms of two parameters, q and q' representing relative size of the rod.

Results of Calculations and Discussions

Let us define the two parameters, q and q', as $q=(R/L)$ and $q'=(L/R)$ so that $q=0$ represents an infinitesimally thin rod, while $q'=0$ represents an infinitesimally thin disc.

As recognized from eq 7, when the value of (hL) and (hR) are small enough, $A(U)$ must be approximated by limiting the order of the series expansion so small as a few orders, as performed by van Aartsen,[10] to give

$$A(U)\cong(8/15)\frac{h^4}{18\cdot 21}\left(\frac{32}{5}L^4-12R^2L^2+\frac{15}{4}R^4\right) \quad (9)$$

That is, when the value of (R/L) is in a range of $0.822<(R/L)<1.588$, the value of $A(U)$ is negative, while the value of (R/L) is out side the range, the value of $A(U)$ is positive. This change of $A(U)$ with (R/L) must be combined with that of $P_i(\cos\omega_0)$ with ω_0 for discussing the shape of the polarized light-scattering patterns.

However, in general, especially when the scattering angle is expanded up to several degrees and the size of the rod is taken as several times larger than the wave length, the values of (hL) and (hR) are no longer so small as to permit the above approximation given by eq 9.

Figure 2 demonstrates such examples of the changes of $A(U)$ with q and q' as keeping the values of L, R, and θ relatively large but realistic for representing the super-structures of crystalline polymers, where the calculations of D_x were performed in accordance to eq 7 by expanding the series as highly as $n=k=100$ to make the expansions fully converged with proper values. As seen in the figure, $A(U)$ decreases with damping oscillations with increases of q and q', but remains still in positive value with

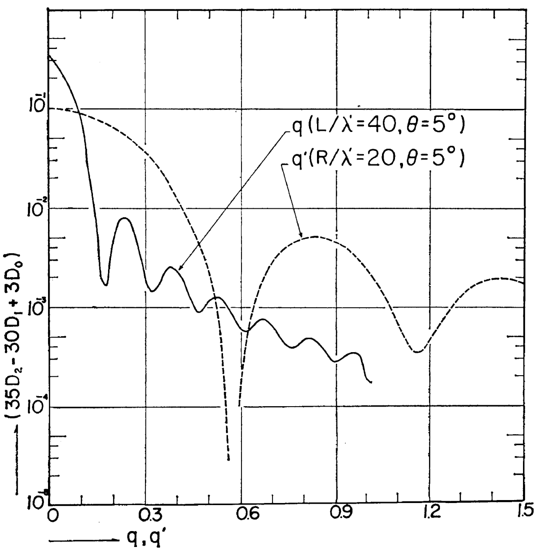

Figure 2. The values of $(35D_2-30D_1+3D_0)$ plotted against the size parameters, q and q', defined by (R/L) and (L/R), respectively.

an exception at $q'=0.5800$, where $A(U)$ becomes a very slightly negative value of -0.303×10^{-4}. This means that the shape of, for example, the H_v pattern is mostly affected by $P_4(\cos\omega_0)$ with the exception at around $q'=0.58$, where the pattern becomes of circular symmetry and opposite of type to that expected only from $P_4(\cos\omega_0)$, because the value of $A(U)$ becomes zero and negative, respectively.

Figure 3 shows the calculated results of the H_v scattering patterns by keeping the length of the rod constant (40 times larger than the wave length), but varying the radius of the rod from infinitesimally thin to half the length and taking the inclined angle of the scattering elements to the rod axis as zero and 50° to make $P_4(\cos\omega_0)$ positive and negative, respectively. In contrast, Figure 4 shows the calculated results of the H_v scattering patterns by keeping the radius of the disc constant (20 times larger than the wave length), but varying the thickness of the disc from infinitesimally thin to half the radius and taking the inclined angle of the scattering elements to the disc axis as zero and 50°.

As is seen in the figures, the H_v patterns taking ω_0 as zero give the $\times$-type pattern, while those taking ω_0 as 50° give $+$-type pattern, in principle, both irrespective of the rod and disc models. The patterns degenerate into small scattering angles with increases of q and q', becoming less distinctive between the $\times$-type and $+$-type patterns and approaching the circular pattern, especially for the rod model. This may be interpreted in terms of the counterbalance of the contributions from the first and second terms in the right-hand side in eq 6 in a previous paper to the total scattering intensity; *i.e.*, rapid decrease of the contribution from the first term, which gives the azimuthal angle dependence of the scattering intensity, in combination with rather slow decrease of the contribution from the second term, which gives no azimuthal dependence of the scattering intensity, both with increases of q and q'.

Figure 5 shows the calculated results of the V_v scattering patterns by keeping the length of the rod constant (40 times larger than the wave length) and the value of p, defined by $p=(b_t/\delta)$, as slightly negative of -0.27 to make the ω_0 dependence of the V_v pattern most obvious, as discussed in a previous paper, but varying the radius of the rod from infinitesimally thin to 20% of the length and taking the inclined angle of the scattering elements to the rod axis as zero, 50°, and 90° to make $P_4(\cos\omega_0)$ positive, negative, and positive again, respectively. Figure 6 shows the calculated results of the V_v scattering patterns by keeping the radius of the disc constant (20 times larger than the wave length) and the value of p as -0.27, but varying the thickness of the disc from infinitesimally thin to 20% of the radius and taking the inclined angle of the scattering elements to the disc axis as zero, 50°, and 90°.

As is seen in the figures, the patterns change, in general, from two-fold symmetry to four-fold symmetry to two-fold symmetry again with the variations of the inclined angle from zero to 50° to 90°, respectively. This must be due, as discussed in a previous paper, to the relative magnitides of the first, second, and the other terms in the right-hand side of eq 7′ in a previous paper to each other; *i.e.*, when the first term is relatively larger the pattern must be of four-fold symmetry; when the second term is predominant the pattern may be of two-fold symmetry; and when the terms other than the

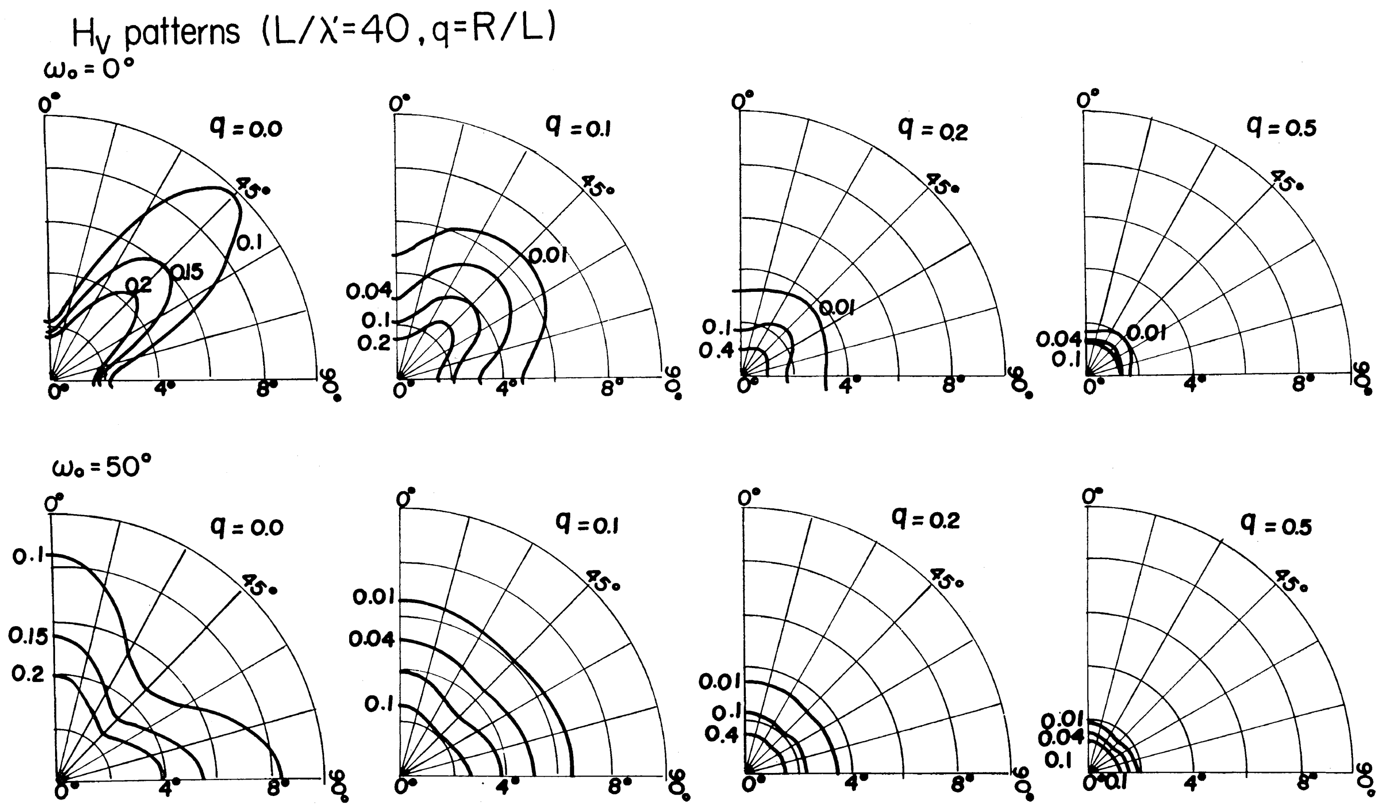

Figure 3. Intensity distribution of H_v scattering calculated by fixing the length of the rod as 40 times larger than the wave length, but varying the radius of the rod from infinitesimally thin to half of the length of the rod and taking the inclined angle of scattering elements to the rod axis as zero and 50°.

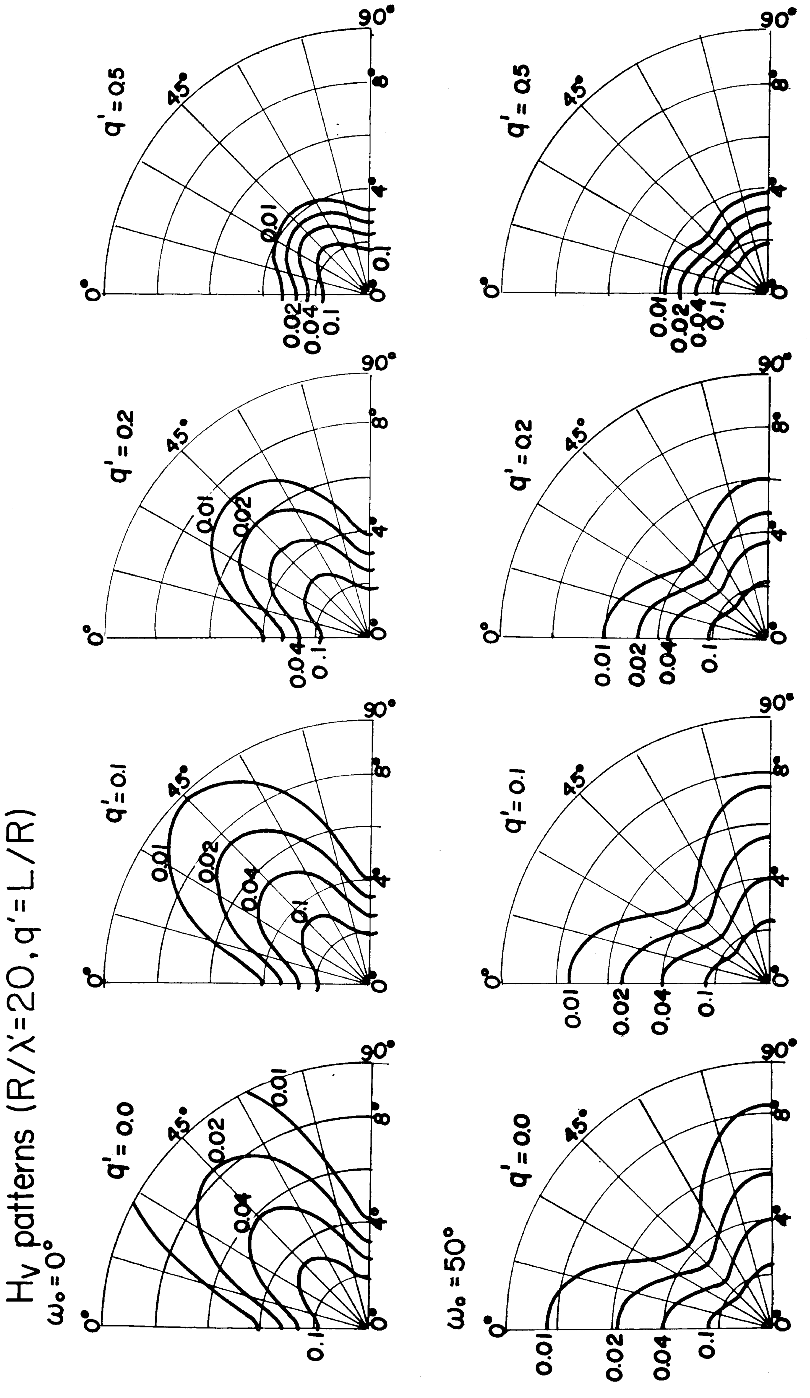

Figure 4. Intensity distribution of H_v scattering calculated by fixing the radius of the disc as 20 times larger than the wave length, but varying the thickness of the disc from infinitesimally thin to half of the radius of the disc and taking the inclined angle of scattering elements to the disc axis as zero and 50°.

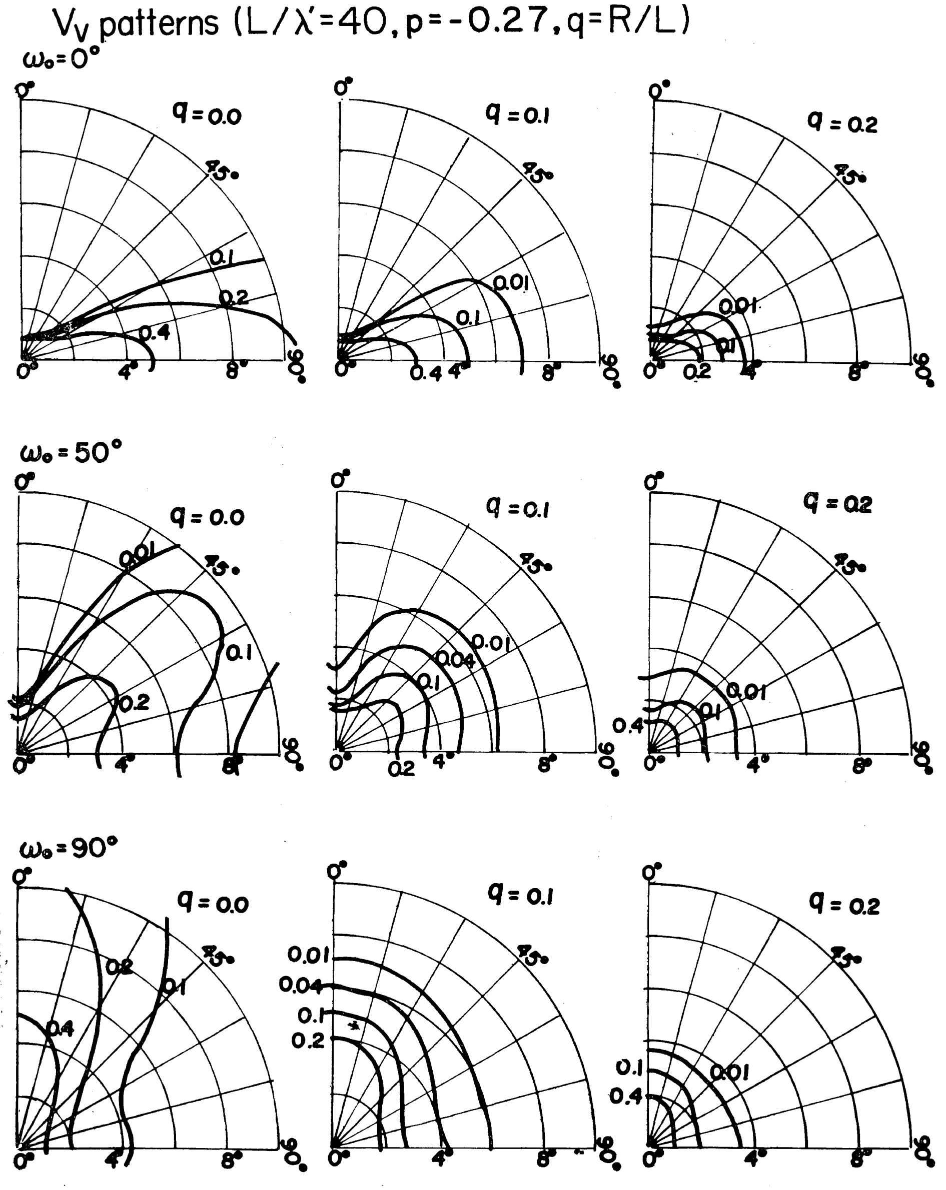

Figure 5. Intensity distribution of V_v scattering calculated by fixing the length of the rod as 40 times larger than the wave length and the value of p as -0.27, but varying the radius of the rod from infinitesimally thin to 20% of the length of the rod and taking the inclined angle of scattering elements as zero, 50°, and 90°.

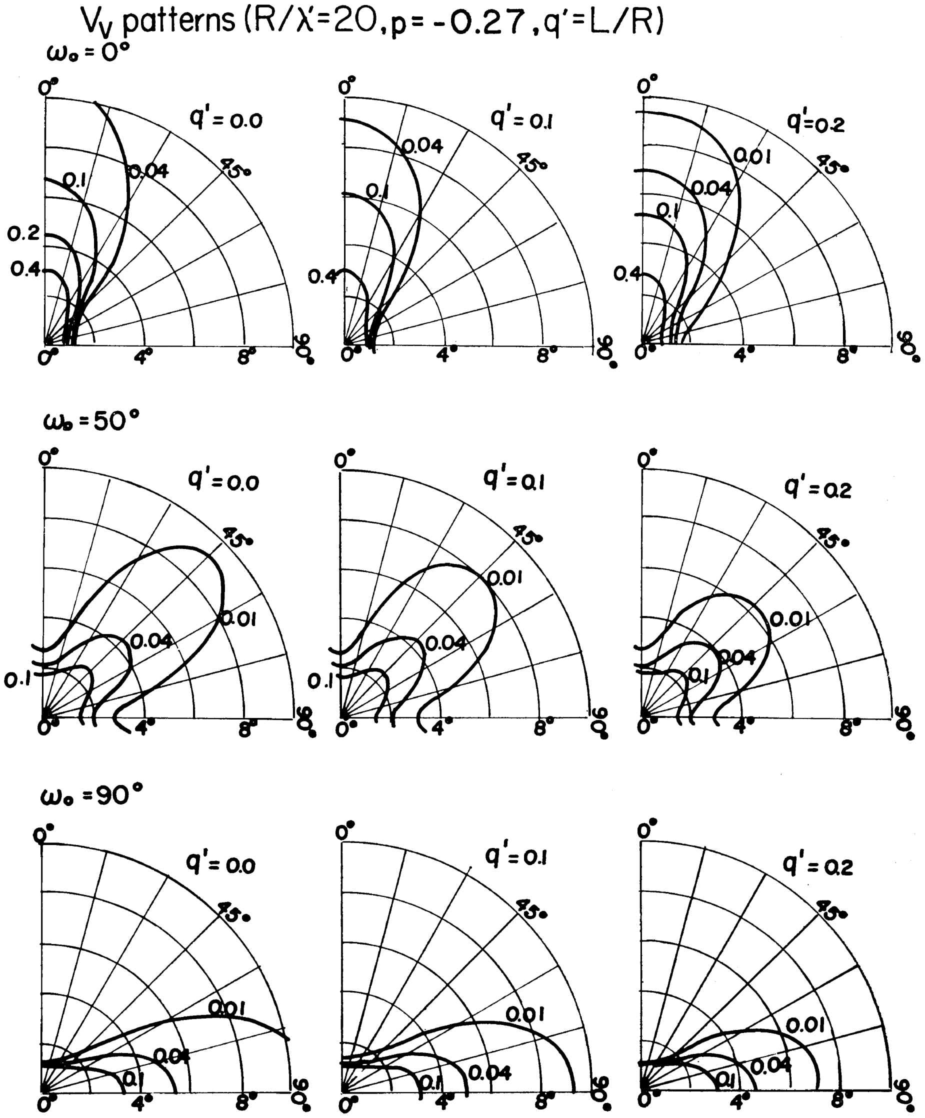

Figure 6. Intensity distribution of V_v scattering calculated by fixing the radius of the disc as 20 times larger than the wave length and the value of p as -0.27, but varying the thickness of the disk from infinitesimally thin to 20% of the radius of the disc and taking the inclined angle of scattering elements as zero, 50°, and 90°.

first and second terms, which are independent of the azimuthal angle, are relatively larger the pattern must be of circular symmetry.

The V_v patterns similar to the results of the H_v patterns, degenerate into small scattering angles, in general, with increases of q and q'. The fact that the ω_0 dependence of the V_v pattern for the rod model is quite opposite to that for the disc model, must be noted in contrast to the above results of the H_v patterns having no distiction between the two models. That is, the V_v patterns for the rod model change from the horizontal dumb-bell to the vertical type, while the V_v patterns for the disc model change from the vertical dumb-bell to the horizontal type, both with increase of ω_0 from zero to 90°. This may be interpreted in terms of the most significant contributions of the q and q' through the second terms in eq 7′ in our previous paper.

REFERENCES

1. M. B. Rhodes and R. S. Stein, *J. Polym. Sci., Part B*, **1**, 663 (1963).
2. J. Borch and R. H. Marchessault, *J. Polym. Sci., Part C*, **28**, 153 (1969).
3. M. Moritani, N. Hayashi, A. Utsuo, and H. Kawai, *Polymer J.*, **2**, 74 (1971).
4. J. Borch, A. Sarko, and R. H. Marchessault, *Bull. Amer. Phys. Soc.*, **16**, 321 (1971).
5. S. Clough, J. J. van Aartsen, and R. S. Stein, *J. Appl. Phys.*, **36**, 3073 (1965).
6. R. Yang and R. S. Stein, *J. Polym. Sci., Part A-2*, **5**, 939 (1967).
7. R. J. Samuels, *J. Polym., Sci., Part A*, **3**, 1741 (1965); *ibid., Part C*, **13**, 37 (1966); *ibid., Part A-2*, **6**, 1101 (1968).
8. M. Motegi, T. Oda, M. Moritani, and H. Kawai, *Polymer J.*, **1**, 209 (1970).
9. R. S. Stein, P. Erhardt, J. J. van Aartsen, S. Clough, and M. B. Rhodes, *J. Polym. Sci., Part C*, **13**, 1 (1966).
10. J. J. van Aartsen, *Eur. Polym. J.*, **6**, 1095 (1970).